PHYSICAL REVIEW A **95**, 062707 (2017)

Vicinage effect in the energy loss of H_2 dimers: Experiment and calculations based on time-dependent density-functional theory

N. E. Koval,[1,*] A. G. Borisov,[2] L. F. S. Rosa,[3] E. M. Stori,[3] J. F. Dias,[4] P. L. Grande,[4]
D. Sánchez-Portal,[1] and R. Díez Muiño[1]

[1]*Centro de Física de Materiales CFM/MPC (CSIC-UPV/EHU) and Donostia International Physics Center DIPC, Paseo Manuel de Lardizabal 5, 20018 San Sebastián, Spain*

[2]*Institut des Sciences Moléculaires d'Orsay, ISMO, Unité de Recherches CNRS-Université Paris-Sud UMR 8214, Bâtiment 351, Université Paris-Sud, F-91405 Orsay Cedex, France*

[3]*Surrey Ion Beam Centre, University of Surrey, Guildford, Surrey GU2 7XH, United Kingdom*

[4]*Instituto de Física da Universidade Federal do Rio Grande do Sul UFRGS, Avenida Bento Gonçalves 9500, 91501-970 Porto Alegre, Rio Grande do Sul, Brazil*

(Received 21 March 2017; published 20 June 2017)

We present a combined theoretical and experimental study of the energy loss of H_2^+ molecular ions interacting with thin oxide and carbon films. As a result of quantum mechanical interference of the target electrons, the energy loss of a molecular projectile differs from the sum of the energy losses of individual atomic projectiles. This difference is known as the vicinage effect. Calculations based on the time-dependent density functional theory allow the first-principles description of the dynamics of target excitations produced by the correlated motion of the nucleons forming the molecule. We investigate in detail the dependence of the vicinage effect on the speed and charge state of the projectile and find an excellent agreement between calculated and measured data.

DOI: 10.1103/PhysRevA.95.062707

I. INTRODUCTION

The study of the stopping processes of light projectiles in matter is essential not only for a basic understanding of particle-solid interactions but also for many applied fields of research, such as plasma physics [1,2], medical therapies [3–5], and radiation damage [6]. The transfer of energy from the incident projectile to the electrons of the target is a very complex problem in which phenomena such as dynamic screening and charge transfer processes have to be considered. Despite this inherent intricacy, the energy loss of a single charged particle in matter is now reasonably well understood. The same situation for a cluster of incident particles, however, requires more detailed investigation.

In the pioneering work of Brandt *et al.* [7], it was shown that the energy loss of an ionic cluster is different from the sum of the energy losses of its individual constituents. In other words, there is an interference among the interactions of the different cluster components with the electrons of the target [8], which is often called the *vicinage effect* [9–16]. From an experimental point of view, the vicinage effect is usually quantified by measuring a stopping power ratio, i.e., the ratio between the stopping power of the cluster or molecule and the sum of the stopping powers of its constituents [17–20].

For sufficiently high projectile energies, the stopping power can be evaluated through linear theory [9,21], which yields very reasonable results. At very low energies, static density functional theory (DFT) can be used to calculate the stopping through the scattering formalism [22,23]. In between these two cases, however, in the regime of intermediate velocities, the accurate description of the energy loss process is much more involved because quasistatic or perturbative approximations break down even for unit-charge projectiles. Only recently, with advances in time-dependent density functional theory (TDDFT), a fully *ab initio* evaluation of the electronic stopping power has become possible for atomic projectiles [24–27].

In this work, we take further advantage of this methodology to analyze the subtle interference effects arising in the energy loss of molecular projectiles moving through matter. We use a real-time propagation approach [28–30] that allows us to calculate the energy loss in the whole range of projectile velocities and provides a very intuitive picture of the complex many-body processes involved. We combine our theoretical results with experimental measurements of the stopping ratio of molecular hydrogen ions interacting with SiO_2, Al_2O_3, and C thin films. The comparison between accurate calculations and empirical information provides a most distinctive image of the vicinage effect in condensed matter.

II. METHODS

A. Theoretical model

We are interested in finite-size systems for which the time scale of the interaction is relatively short and there is no appreciable variation in the internuclear distance among the constituents of the incident projectile. This is realized by the present experimental conditions of H dimers impinging on ultrathin films. In our theoretical treatment, we apply the Kohn-Sham (KS) scheme of TDDFT to calculate the energy loss of the molecular projectile colliding with a spherical cluster representing the target. A sketch of the system is shown in Fig. 1. The distance between the two protons in the dimer is fixed and equals $d = 2$ a.u., corresponding to the equilibrium bond length of H_2^+ in the gas phase. The velocity v of the projectiles is kept constant during the time evolution. The angle Θ between the axis connecting the two protons and the direction of motion determines the orientation of the dimer.

*natalia_koval@ehu.eus

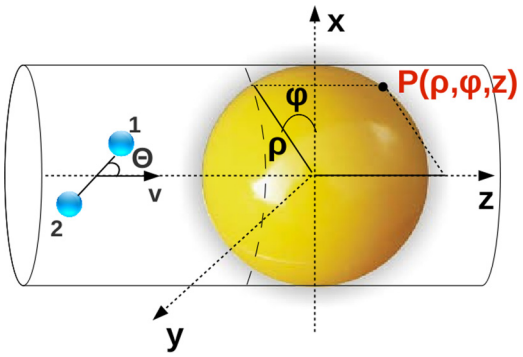

FIG. 1. Sketch of the system for TDDFT calculations. The cluster-projectile system is represented on the three-dimensional cylindrical grid where each point P is characterized by coordinates (ρ,ϕ,z). A hydrogen dimer moves along the z axis with a constant velocity υ and crosses the spherical cluster through the geometrical center. The angle Θ is constant.

The time evolution of the electronic density of the system during the collision process is obtained by solving time-dependent KS equations [31]:

$$i\frac{\partial}{\partial t}\psi_j(\mathbf{r},t) = [T + V_{\rm eff}(\mathbf{r},t)]\psi_j(\mathbf{r},t). \quad (1)$$

The effective potential includes four terms, $V_{\rm eff}(\mathbf{r},t) = V_{\rm ext}(\mathbf{r},t) + V_{\rm H}(\mathbf{r},t) + V_{\rm xc}(\mathbf{r},t) + V_{\rm p}(\mathbf{r},t)$, where $V_{\rm ext}$ is the external potential created by the cluster positive background, $V_{\rm H}$ is the Hartree potential created by the electronic density, and $V_{\rm xc}$ is the exchange-correlation potential of Gunnarson and Lundqvist (GL) [32] within the adiabatic local density approximation (ALDA). Finally, $V_{\rm p}(\mathbf{r},t)$ is the potential of the projectile (created by one or two protons depending on the problem). The time-dependent electron density is given by $n(\mathbf{r},t) = \sum_{j=\rm occ} |\psi_j(\mathbf{r},t)|^2$, where the sum runs over all occupied KS orbitals $\psi_j(\mathbf{r},t)$. The details of similar time-dependent calculations can be found elsewhere [28–30,33]. Note, however, that in the present case the three-dimensional (3D) problem is considered in cylindrical coordinates ($r = \rho,\phi,z$) because of the reduced symmetry.

The initial condition for the time propagation of the KS orbitals $\psi_j(\mathbf{r},t=0)$ is set by the KS orbitals of the unperturbed projectile and target at large separations prior to the collision. To this end, the ground state of the hydrogen dimer and that of the cluster are calculated separately within the density functional theory (DFT) [34] in the local density approximation (LDA) with GL exchange-correlation potential. The KS equations [35] are solved self-consistently. The cluster is represented in the spherical jellium model (SJM) [36] defined by the Wigner-Seitz radius $r_{\rm s}$ and the cluster radius $R_{\rm cl}$. Thus, we represent each experimental target by a given value of $r_{\rm s}$, which corresponds to the effective electron density $n_{\rm eff} = (4\pi r_{\rm s}^3/3)^{-1}$ and can be obtained from the observed plasma frequency, $\omega_{\rm p} = \sqrt{4\pi n_{\rm eff}}$ [18].

The average energy loss is calculated by integrating the Coulomb force acting on the projectile over the whole trajectory, $E_{\rm loss} = -\upsilon \int_0^\infty F_{\rm z}(t)dt$. The stopping power is defined as the average energy loss per unit path length inside the cluster, $S = E_{\rm loss}/(2R_{\rm cl})$. The stopping power ratio is calculated as the ratio between the stopping power of a molecular projectile and twice the stopping power of an atomic projectile, $R = \frac{S_{\rm H_2}}{2S_{\rm H}}$.

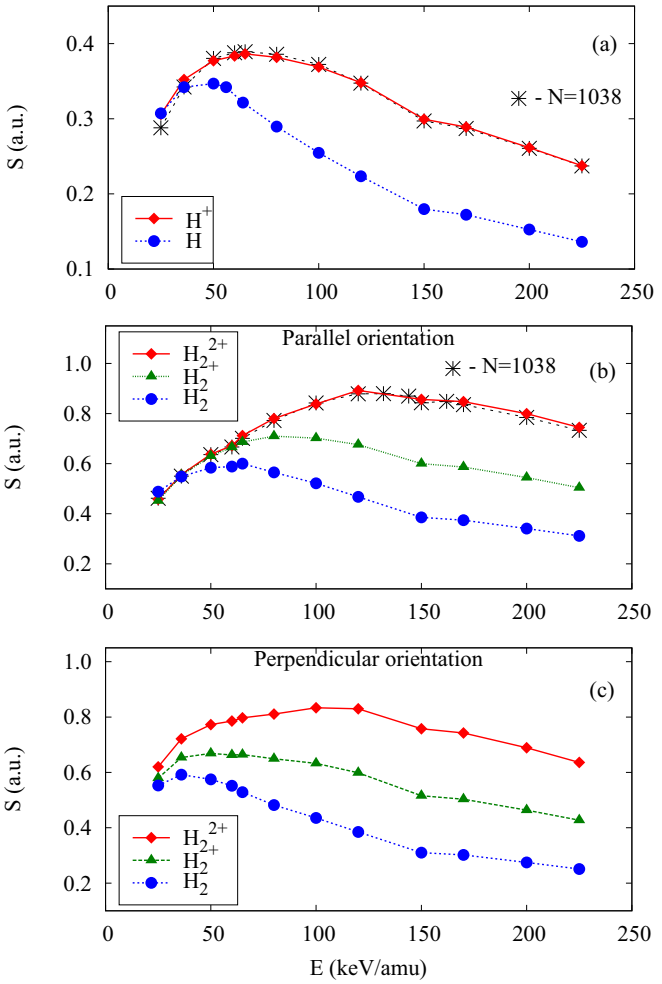

FIG. 2. Stopping power, S, as a function of the projectile energy for the hydrogen in different initial charge states for (a) hydrogen atom; (b) hydrogen dimer in parallel orientation; and (c) hydrogen dimer in perpendicular orientation. Results are shown for fully ionized (◆ and ∗), partially ionized (▲) and neutral (●) species.

Let us make a remark concerning the representation of the target by a finite-size spherical particle, with a geometry different from the experimental one (thin film). Comparing results obtained for different cluster sizes, with $N = 338$ ($R_{\rm cl} = 5.75$ Å) and $N = 1038$ electrons ($R_{\rm cl} = 8.37$ Å), we have obtained [see Fig. 2(a) and 2(b)] that the calculated S and R values converged to better than 1% for both clusters. This implies that the results are representative of the bulk processes both for theory and experiment since the ingoing and outgoing trajectory path, as well as the surface crossing, gives only a small contribution [24]. Moreover, this indicates that the energy loss process, as well as the correlation between nucleons, is determined by the short-range rearrangements of the electron density and that the electron wake potential at this scale is very similar for small finite-size objects and for an infinite solid. In what follows, the theoretical results will be shown for the cluster with $N = 338$ electrons ($r_{\rm s} = 1.56$ a.u. is used in the calculations).

B. Experimental procedure

Thin films with similar r_s values (Al_2O_3 and C, $r_s = 1.6$ a.u.) were used to measure the vicinage effect. Results for a SiO_2 target ($r_s = 1.56$ a.u.) previously published in Ref. [18] will be shown as well. The C film was deposited via filtered cathodic vacuum arc (FCVA) [37] on Si ⟨100⟩ with a native film of SiO_2 on the top. The Al_2O_3 film was deposited above a carbon substrate via RF magnetron sputtering (AJA Orion-8). In these experiments, only films thinner than 50 Å were used. The films were mounted on a three-axis goniometer of the Medium Energy Ion Scattering (MEIS) facility at the Ion Implantation Laboratory (LII), at UFRGS. The chamber containing the samples was connected to a 500-kV electrostatic accelerator manufactured by HVEE, which provided a stable H^+ and H_2^+ beam with energies from 50 up to 200 keV/amu, with current between 5 and 20 nA along the sample normal. The backscattered H^+ ions emerging from the target were analyzed using a toroidal electrostatic analyzer (TEA) mounted at 120 deg with respect to the beam direction. The TEA angular aperture is 24 deg and each angle bin corresponds to 0.08 deg. The overall energy resolution of the system is 300 eV for 100 keV H^+ beam. The two-dimensional (2D) map of ion scattering intensities as a function of scattered energy and angle was then analyzed using the procedure described in Refs. [18,38].

III. RESULTS AND DISCUSSION

When studying the interaction of projectiles with matter it is important to take into account the charge state of the projectile [9,39]. Once the energetic hydrogen ion H_2^+ enters the solid, it may get stripped of its bound electron and dissociate (due to the so-called Coulomb explosion) after passing the very first atomic layer [40,41]. Since in our case the target material is a thin film of less than 50 Å, the distance between the fragments to dissociate does not increase significantly and the two fragments move together. This justifies the use of a fixed distance between the protons in the dimer in our calculations.

There are three possible charge states for the molecule, H_2^0, H_2^+, and H_2^{2+}, and two possible charge states, H^0 and H^+, for the atom moving inside the solid. To access the role of the charge state of the projectile in the dynamic screening, energy loss, and vicinage effect we performed calculations of the stopping power for neutral and ionic projectiles impinging at the cluster. The corresponding results are shown in Fig. 2 for incident atoms and molecules. In the latter case, two orientations of the hydrogen dimer, parallel ($\Theta = 0°$) and perpendicular ($\Theta = 90°$) to the direction of motion, have been considered. As the main observation from Fig. 2, the stopping power shows a pronounced charge-state dependence in particular for swift projectiles. As the projectile charge increases, the friction force gets stronger and the stopping power maximum is shifted to higher projectile energies. As for the hydrogen dimer, along with the charge state, the stopping power also depends on the orientation of the molecular axis, which is one of the consequences of the vicinage effect, as we discuss further in this paper.

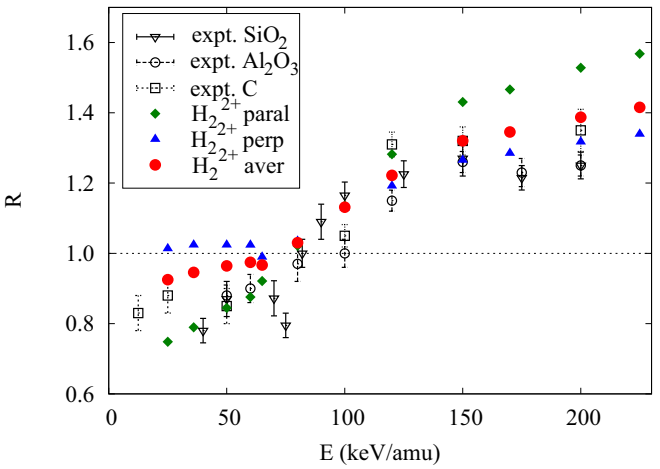

FIG. 3. Stopping power ratio, R, for H_2^{2+} as a function of the projectile energy. Calculated stopping ratio for the dimer moving in parallel (◆), perpendicular (▲), and averaged (●) orientations through the jellium cluster with $r_s = 1.56$ a.u. Experimental stopping ratio for randomly oriented hydrogen ions in SiO_2 (▽), Al_2O_3 (○) and carbon C (□) thin films.

The charge-state dependence of the calculated stopping power decreases for low projectile energies and nearly falls on a unique curve below 40 keV per nucleon. This indicates that the total electron density around the projectile is very similar once inside the spherical nanocluster, i.e., the memory on the initial charge state is lost. Indeed, owing to the fast electron capture and loss processes, one would expect that the equilibrium charge state should be promptly reached by the projectile moving within the electron gas. For hydrogen projectiles interacting with a solid, this equilibrium charge state is known to be strongly energy dependent. Both for atomic and molecular hydrogen at energies above 40 keV, the fully ionized fractions dominate, reaching 100% at about 200 keV. Below 40 keV, the neutral fractions dominate [40,42]. The discussion above leads to the conclusion that irrespective of the initial charge state, similar stopping powers should be found within a broad energy range. Figure 2 shows that in our TDDFT calculations this is only the case for low energies where ionized projectiles become neutralized via electron capture. At high energies, neutral projectiles do not reach the ionized state. This inaccuracy in our calculation is partially due to the small size of the cluster and thus to a too short interaction time, as well as to the intrinsic flaws of standard local and semilocal exchange-correlation terms to properly describe the electron ionization processes.

At low energies, the most relevant initial charge states from the experimental point of view are the neutral H atom and the neutral H_2 molecule. Taking into account, however, that at low energies the equilibrium charge state is reached in present TDDFT calculations and the stopping powers for both neutral and fully ionized projectiles are the same (Fig. 2), the most reasonable choice is to use H^+ and H_2^{2+} as projectiles in our calculations for the whole range of energies considered.

In Fig. 3, we compare the calculated and measured stopping power ratio as a function of the incident kinetic energy for

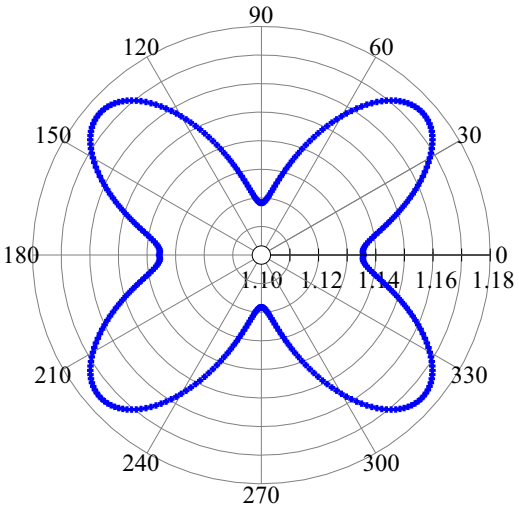

FIG. 4. Polar plot of the stopping power ratio, R, for $H_2{}^{2+}$ moving with velocity 2 a.u. as a function of angle Θ of the orientation of the dimer relative to the direction of motion.

the hydrogen dimer interacting with SiO_2, Al_2O_3, and C. Because of the similarity of the Wigner-Seitz parameter r_s for these different materials, only the TDDFT data for $r_s = 1.56$ (relevant for SiO_2) are shown in the figure. The results for r_s values corresponding to alumina and carbon are very similar, as can be also inferred from the experimental data. Once averaged over all possible orientations of the dimer, the theoretical result closely matches the experimental data in the absolute value and in the energy of the transition from negative $R < 1$ (low energies) to positive $R > 1$ (high energies) interference between the nucleons. In the present TDDFT calculations, the projectile kinetic energy for which the transition occurs is shifted by roughly 50 keV from the one that would be obtained in a simpler linear theory description of the interference effect. In the latter case, the critical projectile velocity υ can be obtained from $\upsilon = 2\omega_p d/\pi$ [7] that corresponds in our case to $E = 32$ keV.

In order to gain further insight into the effect of the correlation between nucleons, we show in Fig. 3 the stopping power ratio calculated for perpendicular and parallel orientations of the molecule with respect to the direction of motion. As one might expect, the vicinage effect is stronger for the parallel orientation where the second nucleon appears in the region of the maximum variation of the induced screening electron density in the wake potential produced by the first nucleon [43]. Observe that at low projectile velocities the vicinage effect is strong for the parallel orientation and vanishes for the perpendicular one. Indeed, the nucleons are efficiently screened and the energy loss is dominated by the electron-hole pair excitations, i.e., binary type collisions with target electrons [23]. The collision events are nearly independent for the perpendicular orientation, while in the parallel orientation the second nucleon experiences the shadow effect from the first one.

The analysis of the effect of molecular orientation is further continued with the help of Fig. 4, where we show the dependence of the calculated stopping power ratio on the orientation of the molecular axis Θ for the $\upsilon = 2$ a.u. case. The perpendicular orientation ($\Theta = 90^\circ$) corresponds to the lowest $R = 1.118$, while the maximum $R = 1.175$ appears at $\Theta = 40^\circ$. Interestingly, for the latter angle, the molecular axis is oriented close to the edge of the Mach cone, as can be inferred from the induced density snapshots shown in Fig. 5.

The analysis of the dynamic screening of projectiles helps to understand the difference in the stopping ratio for different orientations. Figures 5(a)–5(c) show the snapshots of the induced electronic density inside the cluster when two protons in different orientations or a single proton are passing through the center of the cluster with velocity 2.5 a.u. (150 keV/amu). The protons move along the z axis from left to right. The induced density is the difference between the electronic density at a given time t and the electronic density at time $t = 0$: $\Delta n(\mathbf{r},t) = n(\mathbf{r},t) - n(\mathbf{r},t = 0)$. This quantity is plotted in the $(\rho,z,\phi = 0)$ plane. The center of the cluster is located at $(\rho = 0, z = 0)$. In Figs. 5(a)–5(c) we see the cone-shaped screening cloud behind each projectile, which means that the projectiles create a wake of induced electronic charge in the target. This form of the cloud is characteristic for projectile velocities which are much higher than the Fermi velocity of electrons ($\upsilon_F = 1.23$ a.u.) in the cluster. Thus, the response of the cluster electrons to the motion of the projectiles is delayed. The second proton in the parallel dimer feels the wake of the first one [Fig. 5(a)]. As a consequence, in this case the stopping power for the second proton in the dimer is larger than the one for the first proton. For the perpendicular orientation of

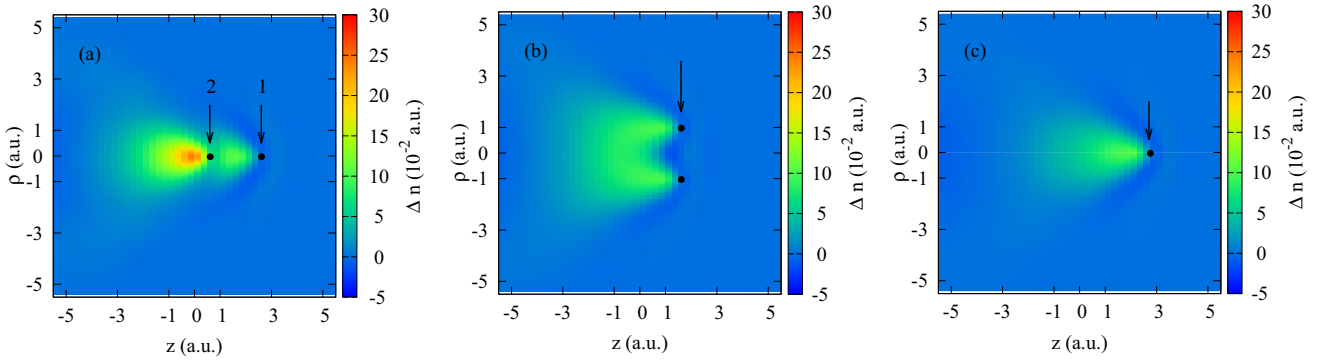

FIG. 5. Snapshots of the induced electronic density in the cluster by the moving projectiles: (a) proton dimer in the parallel orientation; (b) proton dimer in the perpendicular orientation; and (c) single proton. Velocity in all the cases is $\upsilon = 2.5$ a.u. Black dots indicate the positions of the protons.

the dimer, the picture is completely different [Fig. 5(b)]: Both protons are screened alike and the screening cloud for each one looks similar to the screening of the single proton [Fig. 5(c)]. Therefore, it is the wake effect in the screening of the parallel dimer that leads to a larger variation of the vicinage effect at high energies. The asymmetry for perpendicular and parallel orientations will then depend on the wake aperture angle.

IV. CONCLUSIONS

In summary, we have demonstrated that our three-dimensional real-time TDDFT approach is able to reproduce almost perfectly experimental results for the stopping power ratio of hydrogen dimers, even though we used a jellium model to study insulating targets. The intricate effects arising in the combined dynamic screening of the two moving nuclei can lead to constructive or destructive interference effects in the electronic stopping, depending on their kinetic energy. Our calculations show that the interference effects are much more important for a dimer whose symmetry axis is parallel to the velocity vector than for a dimer with perpendicular orientation, due to the wake created by the proton traveling ahead. The agreement between the theoretical results and the experimental measurements is particularly remarkable for the energy regime in which $R < 1$, where linear theory is unable to reproduce even the qualitative trend [18]. A nonperturbative method like TDDFT is thus shown to be a powerful theoretical tool to describe the electronic stopping power of complex projectiles over the full range of kinetic energies.

ACKNOWLEDGMENTS

This work was partially supported by the Basque Departamento de Educación, Universidades e Investigación, the University of the Basque Country UPV/EHU (Grant No. IT-756-13) and the Spanish Ministerio de Economía y Competitividad (Grants No. FIS2016-76471-P and No. MAT2016-78293-C6-4-R). We are indebted to the Brazilian agencies CAPES, CNPq, and FAPERGS for partial support of the experimental part of this work.

[1] J. A. Frenje, P. E. Grabowski, C. K. Li, F. H. Séguin, A. B. Zylstra, M. G. Johnson, R. D. Petrasso, V. Y. Glebov, and T. C. Sangster, Phys. Rev. Lett. **115**, 205001 (2015).
[2] M. D. Barriga-Carrasco, D. Casas, and R. Morales, Phys. Rev. E **93**, 033204 (2016).
[3] S. Limandri, P. de Vera, R. C. Fadanelli, L. C. C. M. Nagamine, A. Mello, R. Garcia-Molina, M. Behar, and I. Abril, Phys. Rev. E **89**, 022703 (2014).
[4] W. D. Newhauser and R. Zhang, Phys. Med. Biol. **60**, R155 (2015).
[5] W. Donahue, W. D. Newhauser, and J. F. Ziegler, Phys. Med. Biol. **61**, 6570 (2016).
[6] A. Lim, W. M. C. Foulkes, A. P. Horsfield, D. R. Mason, A. Schleife, E. W. Draeger, and A. A. Correa, Phys. Rev. Lett. **116**, 043201 (2016).
[7] W. Brandt, A. Ratkowski, and R. H. Ritchie, Phys. Rev. Lett. **33**, 1325 (1974).
[8] N. R. Arista, Phys. Rev. B **18**, 1 (1978).
[9] P. M. Echenique, F. Flores, and R. H. Ritchie, Solid State Phys. **43**, 229 (1990).
[10] N. R. Arista, NIMB **164**, 108 (2000).
[11] R. Díez Muiño and A. Salin, Phys. Rev. B **62**, 5207 (2000).
[12] Z. L. Mišković, S. G. Davison, F. O. Goodman, W.-K. Liu, and Y.-N. Wang, Phys. Rev. A **63**, 022901 (2001).
[13] M. Alducin, R. Díez Muiño, J. I. Juaristi, and P. M. Echenique, Phys. Rev. A **66**, 054901 (2002).
[14] S. Heredia-Avalos and R. Garcia-Molina, Phys. Rev. A **76**, 032902 (2007).
[15] I. Nagy and I. Aldazabal, Phys. Rev. A **81**, 052901 (2010).
[16] P. Sigmund and A. Schinner, Eur. Phys. J. D **61**, 39 (2011).
[17] R. C. Fadanelli, P. L. Grande, M. Behar, J. F. Dias, K. Czerski, and G. Schiwietz, Phys. Rev. B **73**, 245336 (2006).
[18] S. M. Shubeita, M. A. Sortica, P. L. Grande, J. F. Dias, and N. R. Arista, Phys. Rev. B **77**, 115327 (2008).
[19] S. M. Shubeita, P. L. Grande, J. F. Dias, R. Garcia-Molina, C. D. Denton, and I. Abril, Phys. Rev. B **83**, 245423 (2011).
[20] A. L'Hoir, C. Cohen, J. J. Ganem, I. Trimaille, I. C. Vickridge, and S. M. Shubeita, Phys. Rev. A **85**, 042901 (2012).
[21] J. Burgdörfer, NIMB **67**, 1 (1992).
[22] P. M. Echenique, R. M. Nieminen, and R. H. Ritchie, Solid State Commun. **37**, 779 (1981).
[23] P. M. Echenique, R. M. Nieminen, J. C. Ashley, and R. H. Ritchie, Phys. Rev. A **33**, 897 (1986).
[24] M. Quijada, A. G. Borisov, I. Nagy, R. Díez Muiño, and P. M. Echenique, Phys. Rev. A **75**, 042902 (2007).
[25] A. V. Krasheninnikov, Y. Miyamoto, and D. Tománek, Phys. Rev. Lett. **99**, 016104 (2007).
[26] J. M. Pruneda, D. Sánchez-Portal, A. Arnau, J. I. Juaristi, and E. Artacho, Phys. Rev. Lett. **99**, 235501 (2007).
[27] A. A. Correa, J. Kohanoff, E. Artacho, D. Sánchez-Portal, and A. Caro, Phys. Rev. Lett. **108**, 213201 (2012).
[28] A. G. Borisov, J. I. Juaristi, R. Díez Muiño, D. Sánchez-Portal, and P. M. Echenique, Phys. Rev. A **73**, 012901 (2006).
[29] A. G. Borisov, J. P. Gauyacq, and S. V. Shabanov, Surf. Sci. **487**, 243 (2001).
[30] E. V. Chulkov, A. G. Borisov, J. P. Gauyacq, D. Sánchez-Portal, V. M. Silkin, V. P. Zhukov, and P. M. Echenique, Chem. Rev. **106**, 4160 (2006).
[31] E. Runge and E. K. U. Gross, Phys. Rev. Lett. **52**, 997 (1984).
[32] O. Gunnarson and B. I. Lundqvist, Phys. Rev. B **13**, 4274 (1976).
[33] N. E. Koval, D. Sánchez-Portal, A. G. Borisov, and R. Díez Muiño, NIMB **317**, 56 (2013).
[34] P. Hohenberg and W. Kohn, Phys. Rev. **136**, B864 (1964).
[35] W. Kohn and L. J. Sham, Phys. Rev. **140**, A1133 (1965).
[36] W. Ekardt, Phys. Rev. B **29**, 1558 (1984).
[37] D. S. da Silva, A. D. S. Côrtes, M. H. Oliveira Jr., E. F. Motta, G. A. Viana, P. R. Mei, and F. C. Marques, J. Appl. Phys. **110**, 043510 (2011).

[38] L. F. S. Rosa, P. L. Grande, J. F. Dias, R. C. Fadanelli, and M. Vos, Phys. Rev. A **91**, 042704 (2015).
[39] M. Peñalba, A. Arnau, and P. M. Echenique, Europhys. Lett. **19**, 45 (1992).
[40] C. D. Denton, I. Abril, M. D. Barriga-Carrasco, R. Garcia-Molina, G. H. Lantschner, J. C. Eckardt, and N. R. Arista, NIMB **193**, 198 (2002).
[41] S. M. Shubeita, R. C. Fadanelli, J. F. Dias, and P. L. Grande, Surf. Sci. **608**, 292 (2013).
[42] M. Bergsmann, W. Raab, G. Schrenk, F. Kastner, R. Díez Muiño, A. Arnau, A. Salin, P. Bauer, and P. M. Echenique, Phys. Rev. B **62**, 3153 (2000).
[43] A. Mazarro, P. M. Echenique, and R. H. Ritchie, Phys. Rev. B **27**, 4117 (1983).